Quantum Electronics **33** (10) 883 – 888 (2003)

CONTROL OF LASER RADIATION PARAMETERS

PACS numbers: 42.55.Px; 42.60.Jf
DOI: 10.1070/QE2003v033n10ABEH002517

Study of the spectral characteristics of a femtosecond Ti : sapphire laser after propagation of its radiation through a tapered fibre

S.N. Bagayev, V.I. Denisov, V.F. Zakharyash, V.M. Klementyev, I.I. Korel', S.A. Kuznetsov, V.S. Pivtsov, S.V. Chepurov

***Abstract*. The method and results of precision measurements of the intermode frequency of a Ti : sapphire laser after the propagation of its radiation through a tapered optical fibre are described. It is shown that the stability of the intermode frequency is impaired by half at short averaging times (10 s) and by a factor of 1.1 at long averaging times (1000 s). The results of investigations of the spectrum of a femtosecond Ti : sapphire laser, which is broadened in a tapered optical fibre are presented. It is shown that, by varying the fibre parameters and the characteristics of input pulses, the envelope of the broadened spectrum can be profiled, which is important for practical applications.**

Keywords: *femtosecond laser, optical fibres, nonlinear optics, supercontinuum.*

1. Introduction

The advent of special optical fibres for broadening the mode spectrum of a femtosecond laser (holey fibres [1, 2] and tapered fibres [3 – 6]) has opened up unique possibilities for the synthesis and measurements of frequencies from the radio to UV spectral range. During the propagation of a femtosecond pulse through such fibres, its spectrum is broadened by more than an octave. If the incident radiation is a continuous train of femtosecond pulses, then the broadened spectrum will be discrete, the distance between its components being exactly equal to the mode interval. Such a strong broadening of a relatively low-power emission spectrum became possible due to a high concentration of radiation in these fibres and the shift of the zero-dispersion point toward the incident radiation frequency.

Great recent efforts are directed to the study of the physical foundations of the broadening of emission spectra in fibres, first of all the origin of nonlinearity determining the broadening of the spectrum, as well as the properties of radiation obtained at the fibre output. The most important is the question whether the stability of the intermode frequency is retained after the propagation of a highly stable femtosecond pulse through the optical fibre. Another question is what are the amplitude-frequency parameters of the output radiation or, in other words, what is the intensity distribution between the components of the broadened spectrum? No less important is the problem of the nature and intensity of noises appearing during the transformation of the spectrum. These problems play a key role in practical applications of holey and tapered optical fibres, for example, in systems for frequency synthesis or in the development of an optical clock.

In this paper, we present the results of the experimental study of a change in the stability of the intermode frequency of a train of highly stable femtosecond pulses from a Ti : sapphire laser after their propagation through a tapered fibre, as well as the experimental and theoretical studies of the envelope of the broadened spectrum.

S.N. Bagayev, V.I. Denisov, V.F. Zakharyash, V.M. Klementyev, I.I. Korel', S.A. Kuznetsov, V.S. Pivtsov, S.V. Chepurov Institute of Laser Physics, Siberian Branch, Russian Academy of Sciences, prosp. akad. Lavrent'eva 13/3, 630090 Novosibirsk, Russia; e-mail: clock@laser.nsc.ru

Received 4 February 2003
Kvantovaya Elektronika **33** (10) 883 – 888 (2003)
Translated by M.N. Sapozhnikov

2. Experimental setup

To study the stability of the intermode frequency, we measured carefully the stability of the intermode frequency (100 MHz) at the fibre input and then at its output. One can assume that the processes of conversion of radiation in the fibre into the red and blue regions are different. To verify this, we divided the output emission spectrum with the help of filters into two regions, in which the stability was then measured.

We have developed and built a device for high-precision measurements of the intermode frequency, in which this frequency is transferred with the help of a synthesiser to the low-frequency region, where the chosen frequency (~ 200 Hz) is measured with a high accuracy. Note that the final aim of the development of the methods and devices for high-precision measurements is the measurement of the absolute optical frequencies with a high accuracy ($10^{-15} - 10^{-16}$) using a femtosecond optical clock. These measurements are based on a comparison of the intermode frequency with the frequency of the microwave hydrogen standard (H standard). The comparison is performed using the device described below.

The scheme of the experimental setup is shown in Fig. 1. The comparison device consists of the H standard and a femtosecond laser, whose intermode frequency is stabilised with the help of an PD2 photodiode and the automatic frequency control by the H standard frequency. The device contains two channels: channel I for the synthesis and filtration of a signal from the H standard and channel II

for the synthesis of a signal from a Ti : sapphire laser. The H standard frequency is converted in channel I to the frequency $F_3 = 20$ MHz without the loss of the frequency characteristics of the H standard. The intermode frequency is converted in channel II with the help of a G3-122 synthesiser to the frequency $F_3^* = 2 \times 10^7 \pm 200$ Hz. A signal measured at the frequency 200 Hz is obtained at the M2 mixer output as a difference frequency produced upon mixing frequencies F_3 and F_3^*. The comparison device is designed so that the frequency F_3 phase locked to the H standard frequency always possesses the characteristics of the H standard. A signal from the femtosecond laser (i.e., from the PD1 photodiode) propagating through channel II contains all the frequency fluctuations of the intermode frequency f_m, which are inherent in the Ti : sapphire laser and are acquired during the propagation of its pulses through a tapered fibre. The output power and emission spectrum of the Ti : sapphire laser were controlled with a power meter and a multichannel spectrum analyser, and the shape of the spectrum broadened in the fibre was measured with a multichannel spectrometer.

The comparison device is capable of testing its efficiency using its own time base, when the frequency 100 MHz from the H standard is fed to the M1 mixer input. During the frequency conversion in the comparison device, the noise is carefully filtered with the help of thermally stabilised (with the accuracy $\sim 0.1\,^\circ$C) quartz oscillators and resonance amplifiers in channels I and II.

The expression for the synthesis of the intermode frequency has the form

$$f_m = F_1 - F_2 + F_3^*/10 = F_1 - F_2 + F_3/10 \pm f_x/10, \quad (1)$$

where $F_1 = 99.5$ MHz; $F_3^* = F_3 \pm f_x$; $f_x \approx 200$ Hz$\pm \delta f_x$; and δf_x includes the frequency fluctuations of f_m. In this case, the relative accuracy of the measurement of f_m can be written in the form

$$\delta f_m/f_m = \delta f_x/(10 f_m), \quad (2)$$

because $\delta F_1, \delta F_2, \delta F_3 \ll \delta f_x$.

Experimental studies consist in the measurements of $\delta f_m/f_m$ for different averaging times at the input and output of the tapered fibre.

3. Experimental results and discussion

At the first stage, we studied the intrinsic frequency noise of the device by feeding a 100-MHz signal from the H standard through channel II instead of a signal at frequency f_m (i.e., the intrinsic time base was used). In this case, a signal at the frequency $f_x^* \approx 200$ Hz$\pm \delta f_x$ being measured (f_x^* is the signal from the H standard) was obtained at the mixer output. The results of measurements of $\delta f_m/f_m$ for different averaging times are: 3.1×10^{-12} for 10 s, 3.4×10^{-13} for 10^2 s, 3.12×10^{-14} for 10^3 s, and 3×10^{-15} for 10^4 s. Therefore, the device allows us to measure the intermode frequencies for the averaging times $10^3 - 10^4$ s with a relative accuracy of $10^{-14} - 10^{-15}$. We studied the stability of the measuring system depending on the time during 24 hours. The results are presented in Fig. 2. One can see that the average value of the measured frequency depends on the averaging time and weakly changes in the night–day interval only for long averaging times. The amplitude fluctuations of the frequency being measured for the same averaging times increase by more than an order of magnitude in the daytime. These fluctuations are suppressed by the comparison device.

It is most important to find out whether the stability of the intermode frequency of a train of highly stable femtosecond pulses is preserved after their propagation through the fibreoptic system. We studied the stability of the intermode frequency f_m of a highly stable femtosecond pulse from a Ti : sapphire laser, which was similar to the laser we described in Ref. [7]. This laser was pumped by all

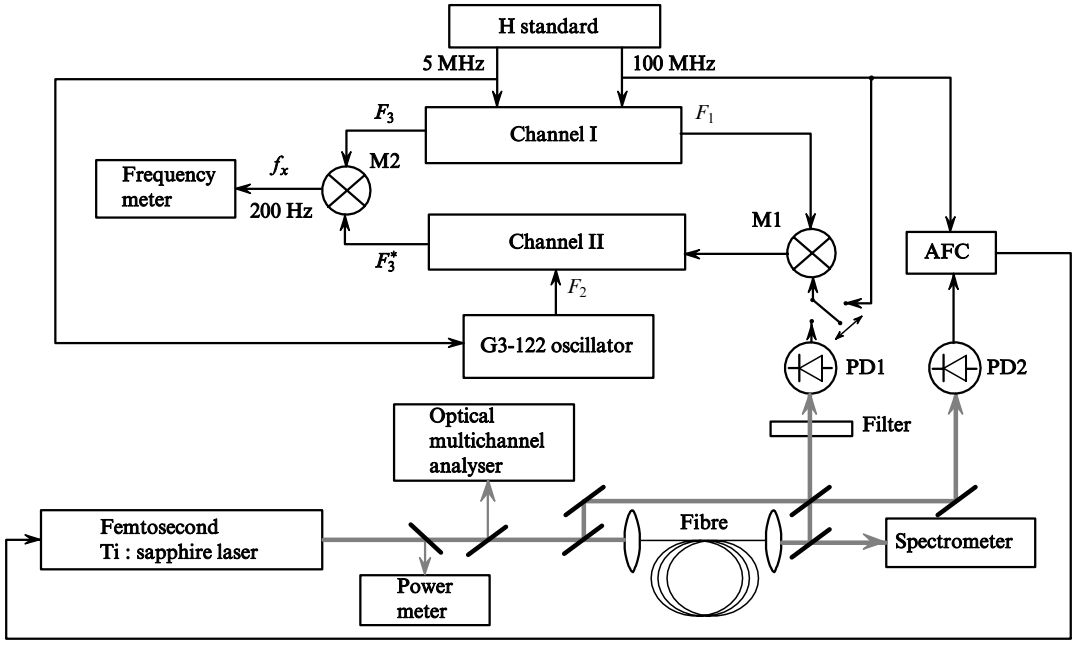

Figure 1. Principal scheme of the experimental setup: (AFC) automatic frequency control; (M1, M2) mixers; (PD1, PD2) photodiodes.

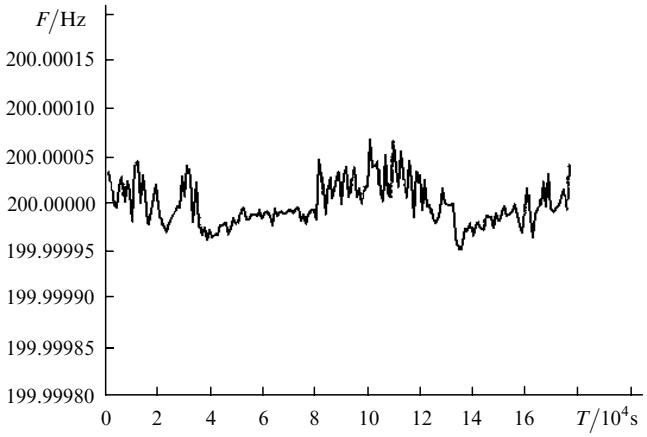

Figure 2. Dependence of the frequency stability of the measuring system on the time during 24 hours (the averaging time is 1000 s).

visible lines from a $\sim$ 7-W continuous-wave argon laser. The femtosecond Ti : sapphire laser had a pulse repetition rate of 100 MHz, an average output power of $\sim$ 350 mW emitted at 810 nm, a pulse duration of 40 fs, and the width of the emission spectrum $\Delta\nu = 20$ nm. We performed a series of measurements at different averaging times at the output of a tapered fibre and then at its input, and vice versa. The results of the measurements are presented in Fig. 3. It follows from the dependences in Fig. 3 that the stability f_m is worse than the stability that can be provided by the measuring system and that the stability f_m drastically changes after the propagation of the pulse through the fibre. At short averaging times, the stability is deteriorated more than twice. As the averaging time increases, the stability improves and it virtually coincides with the stability at the tapered fibre input when the averaging time is equal to 1000 s.

We also studied the dependence of the stability f_m on the region of the broadened spectrum. We divided the spectrum with the help of optical filters into two regions and measured the stability f_m at the fibre output in each of these regions. The results are presented in Table 1, where the result of

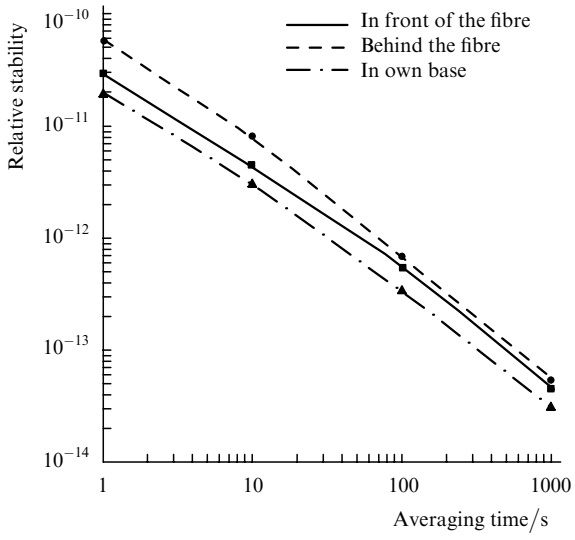

Figure 3. Stability of the intermode frequency.

Table 1.

Experimental conditions	Number of measurements	Root-mean-square deviation (Hz) for the averaging time 100 s
In front of a fibre	98	5.738×10^{-5}
Behind a fibre, $\lambda = 400 - 650$ nm	92	6.940×10^{-5}
Behind a fibre, $\lambda = 700 - 1000$ nm	83	8.458×10^{-5}

measurements made at the fibre input is also given for comparison. It follows from Table 1 that the noise increases asymmetrically during the transformation, being greater in the long-wavelength region.

As mentioned above, we pay a special attention in this paper to the study of physical factors affecting the envelope of the broadened spectrum. We studied experimentally the envelope of the broadened spectrum of a train of femtosecond pulses at the output of tapered optical fibres. About 30 % of the incident radiation power were coupled into the fibre. According to our estimates, the pulse duration in front of the fibre waist was 160 fs, i.e., the pulse acquired a strong chirp after propagation through optical elements and the initial (before tapering) part of the fibre. We studied fibres with the same taper waist length (90 mm) but with different diameters (2, 2.5, and 3 μm). We found some properties of the envelope of the spectrum that were not observed earlier (see solid curves in Fig. 4): all the fibres exhibit the long-wavelength maximum at 970 nm; fibres with the waist diameter $d = 2.5$ μm have a weak maximum at the incident radiation wavelength and one or several short-wavelength maxima; fibres with $d = 2$ and 3 μm have the most intense maximum at the incident radiation wavelength and very weak short-wavelength maximum. Therefore, in fibres with $d = 2.5$ μm, unlike fibres with $d = 2$ and 3 μm, the incident radiation energy is efficiently transferred to the periphery of the broadened spectrum.

These results differ from the results obtained in Refs [3, 5], where the maxima of the envelope of the spectrum are strongly flattened. This difference can be explained by the fact that the peak power of pulses coupled to the fibre waist in papers [3, 5] was substantially lower. In addition, in Ref. [5] a fibre with a taper waist length of 14 cm manufactured by a different method was used.

4. Theoretical analysis

The problem of the formation of the spectrum of a train of ultrashort pulses propagated through an optical fibre can be considered both in the pulse (temporal) and frequency domain representation. In the first case, the spectrum of a train of ultrashort pulses is considered based on the Fourier analysis of the corresponding time series [8 – 10] at the fibre output. The propagation of a pulse in the fibre is described in a traditional way by considering the interaction of this pulse with a nonlinear medium having dispersion properties [11]. Note here that this approach assumes that pulses are identical and the interval between pulses is stable because the presence of any fluctuations leads to the difference between the envelopes of the spectra of a train of ultrashort pulses (experimental data) and an individual pulse (theoretical model). The influence of the stability on the spectral parameters of such pulsed processes (in particular, on the envelope) was considered in detail in Refs [9, 10].

The second approach uses the representation of a train of ultrashort pulses by a polychromatic field, i.e., the evolution of the components of the discrete spectrum during their propagation in a medium is studied within the framework of the initially chosen spectral approach. In experiments on the spectral broadening of a train of femtosecond pulses in fibres, the discrete spectrum consists of a great number of harmonics, and huge computational resources are required to solve this problem exactly. For this reason, we used the first approach for the theoretical description of the spectrum with known experimental parameters.

The broadening of the spectra of ultrashort pulses (generation of a supercontinuum) is usually associated either with self-phase modulation or with the regime of a combined formation of fundamental solitons and non-soliton radiation [12]. The latter regime is observed in the region of anomalous dispersion and is typical for holey fibres in the case of a relatively low radiation power coupled into the fibre [13]. In the tapered fibres under study, the soliton regime, as a rule, has no time to develop because nonlinear effects dominate over dispersion ones due to a high energy density and low dispersion. Thus, the dispersion length L_d of fibres we used in our experiments (a few tens of centimetres) was much longer than the taper waist length (9 cm), whereas for the peak radiation power at the waist equal to 10 kW the nonlinear length was $L_{nl} = 6 \times 10^{-2}$ cm. The broadening of the spectrum under such conditions is caused by self-phase modulation. The spectral broadening coefficient can be estimated from the ratio of the active-region length to the nonlinear length $z/L_{nl} \approx 100$, which agrees with the experimental spectra, whose width for a train of 160-fs pulse propagated through a fibre was up to 350 THz.

Generally speaking, the minimal group-velocity dispersion (GVD) is a necessary condition for obtaining the maximum spectral broadening, because otherwise the GVD will cause an increase in the pulse duration, thereby narrowing down the spectral interval. Although the dispersion length for the fibres we studied is much greater than the taper waist length, dispersion effects nevertheless play a substantial role in the formation of the spectral envelope. For example, one of the nonlinear effects – the formation of the envelope shock wave [14] depends to a great degree on the dispersion profile. This is explained by the fact that the shock wave formed at the trailing edge of the pulse, to which the blue region of the spectrum corresponds, can be weakened due to the dispersion broadening of the temporal profile.

We studied the formation of the envelope of the spectrum of a train of femtosecond pulses using the known standard nonlinear Schrödinger equation [11] describing the propagation of a single pulse in a nonlinear medium

$$\frac{\partial u}{\partial z} + \frac{\mathrm{i}}{2}\frac{\beta_2}{T_p^2}\frac{\partial^2 u}{\partial \tau^2} - \frac{1}{6}\frac{\beta_3}{T_p^3}\frac{\partial^3 u}{\partial \tau^3}$$

$$= \mathrm{i}\gamma P_0\left[|u|^2 u + \frac{2}{\omega_0 T_p}\frac{\partial(|u|^2 u)}{\partial \tau} - \frac{T_R}{\tau}\frac{\partial |u|^2}{\partial \tau}u\right], \qquad (3)$$

where $\gamma = n_2\omega_0/(cA_{eff})$ is the nonlinearity parameter related to the effective mode area A_{eff} and nonlinear refractive index n_2; P_0 is the peak power; T_p is the pulse duration; T_R is the parameter related to the slope of the SRS gain line; and β_i is the ith order dispersion. Nonlinear terms in the right-hand side of (3) describe (from left to right) self-phase modulation (Kerr nonlinearity), the envelope shock wave, and stimulated Raman self-scattering, respectively. The numerical solutions of this equation, taking into account experimental parameters, were found by the Fourier split method [15], which considers independently nonlinear and dispersion effects on a small spatial step l satisfying the inequality $l < L_{nl} < L_d$. In this case, to find the exact profiles of femtosecond pulses, it is important to take into account all the nonlinear effects, including the development of the envelope shock wave and SRS with the second- and third-order dispersion effects. An important advantage of the Fourier split method (except the calculation speed, which is substantially higher than that in difference schemes due to the use of the fast Fourier transform) is the possibility of taking into account the GVD profile in the frequency-domain representation, because the GVD is substantially different at different wavelengths for the

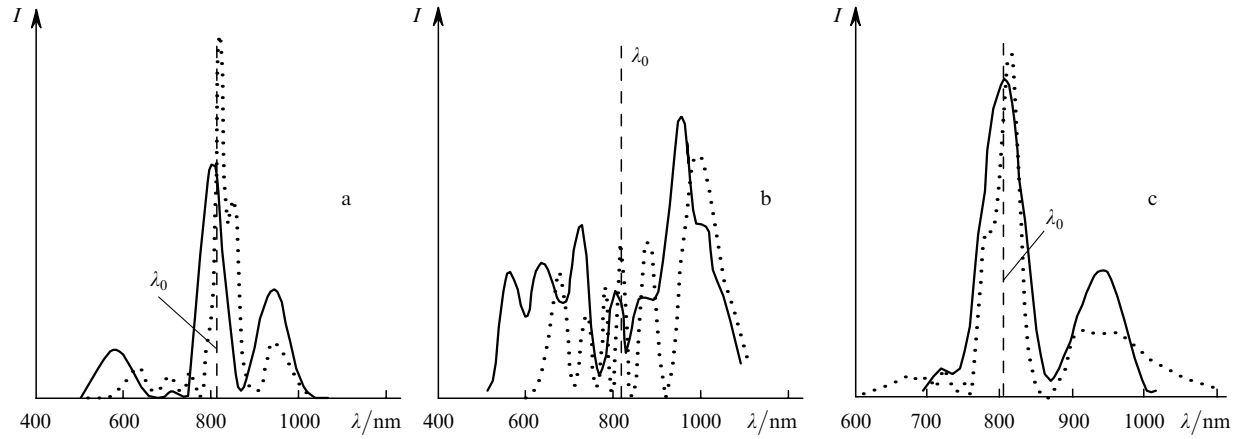

Figure 4. Envelopes of the broadened spectra of a train of femtosecond pulses obtained for the nonlinear length $L_{nl} \approx 0.6$ mm, the waist diameter $d = 2$ (a), 2.5 (b), and 3 μm (c), and the zero-dispersion wavelength $d = 680$ (a), 790 (b), and 900 nm (c). Solid curves are the experiment, the dashed curves are theoretical estimates for pulses having the hyperbolic cosecant shape (dependences of L_d on the waist diameter d were taken from Ref. [3]). All the curves are normalised to the area.

broad spectra of femtosecond pulses both at the fibre input and output [4].

One can see from Fig. 4 that our experimental data agree as a whole with numerical calculations. Some asymmetry of the spectra is explained by the influence of the complicated GVD profile, in which higher dispersion orders should be taken into account, and by the processes of formation of the envelope shock wave and Raman self-scattering. The shape of the spectral envelope, determined by nonlinear and dispersion effects, is very sensitive to these differences. Thus, for $d = 2$ μm (Fig. 4a), the zero-dispersion point lies in the blue region with respect to the central wavelength. Therefore, the effect of the GVD proves to be weaker in this region, and a considerable broadening of the spectrum can be expected compared to the red region [16], which is caused by the formation of the envelope shock wave. The characteristic length of formation of the envelope shock wave under our experimental conditions is about of 3 cm. Therefore, this effect should be taken into account when the waist diameter is comparable to $d = 2$ μm.

In the experiment with $d = 3$ μm (Fig. 4c), the zero-dispersion point is located on the other side of the central frequency, and broadening caused by an increase in the slope of the shock wave front disappears because, as the trailing edge steepness increases, the dispersion terms, which are proportional to the time derivatives, begin to play a substantial role in equation (3). It is the case when the nonzero GVD efficiently prevents the shock wave formation. At the same time, spontaneous Raman self-scattering can be observed in the spectrum [17], which is caused by the fact that the blue spectral components can be treated as pumping lines for the red components in the classical SRS model.

Note here that such a mechanism begins to work for femtosecond pulses before the onset of spectral broadening caused by other nonlinearities because the spectral width of the incident pulse (20 THz at the 0.1 level) already exceeds the Raman shift (about of 13 THz in glasses), while the efficiency of this mechanism is caused by high power densities at the waist (above 100 GW cm^{-2}). In Fig. 4b, the waist diameter is $d = 2.5$ μm and the zero-dispersion point coincides approximately with the central radiation frequency. The spectrum in Fig. 4b covers a broad region and has the intense maxima at the periphery. The spectral parameters of a fibre with such a waist diameter are described by three nonlinear effects: self-phase modulation, which broadens the spectrum, and SRS and a shock wave, which act oppositely to each other (SRS shifts the spectrum to the red, whereas the shock wave shifts the spectrum to the blue). In addition, the pulse shape at the waist input plays a very important role. It is determined not only by the laser parameters but also by the method of radiation coupling into the fibre and the fibre properties (in particular, by the characteristics of the region of transition to the fibre waist), which should be investigated separately.

Generally speaking, the spectra broadened in tapered fibres exhibit typically minima and maxima [18], and in some cases (see Fig. 4b) the spectra have a very complicated structure. A stable signal at the specified frequency can be obtained by varying the parameters of coupled radiation (first of all, the pulse power and shape) and of fibres themselves (diameter and length of the waist). In addition, such a signal can be obtained by locking the central radiation frequency to the dispersion profile of the fibre, the rest of parameters being fixed. However, a comparison of the experimental data with calculations shows that in any case, to obtain an optimal signal at the given frequency, it is necessary to take into account all nonlinear and dispersion effects considered above.

5. Conclusions

We have obtained in this paper the following results. The comparison device has been developed and built for high-precision measurements using a femtosecond optical clock. We have studied the stability of the intermode frequency after the propagation of a train of highly stable ~ 40-fs pulses through the tapered fibre. Our experiments have shown that the short-term stability of the intermode frequency at the fibre output is strongly reduced, but as the averaging time increases, the stability becomes almost equal to the stability at the fibre input. This means that phase fluctuations occur during the transformation of the spectrum, which reduce the short-term stability of the intermediate frequency. The effect of these fluctuations disappears almost completely at long averaging times. We have also found that the stability of the intermode frequency depends on the region of the broadened mode spectrum, being noticeably higher in the short-wavelength region than in the long-wavelength region. Therefore, a tapered fibre can be used in an optical clock and synthesisers.

The theoretical analysis of our results has shown that, except self-phase modulation responsible for the spectral broadening, other nonlinear effects (formation of the envelope shock wave and stimulated Raman self-scattering) and dispersion effects substantially determine the spectral envelope for all the fibres studied. The formal features of these effects can be absent. For example, the additional spectral broadening in the blue region caused by the envelope shock wave may not be manifested because of its compensation by dispersion (for the waist diameter $d = 3$ μm). We have shown that, by varying the fibre parameters and the characteristics of radiation coupled to the fibre, we can profile the envelope of the broadened spectrum, which is important for practical applications.

Acknowledgements. The authors thank T.A. Birks, W.J. Wadsworth, and P.St.J. Russel (University of Bath, United Kingdom) for placing tapered fibres at our disposal. This work was supported by the Russian Foundation for Basic Research (Grant No. 03-02-17114) and INTAS (Grant No. 99-1366).

References

1. Knight J.C., Birks T.A., Russell P.St.J., Atkin D.M. *Opt. Lett.*, **21**, 1547 (1996).
2. Zheltikov A.M. *Usp. Fiz. Nauk*, **170**, 1203 (2000).
3. Birks T.A., Wadsworth W.J., Russell P.St.J. *Opt. Lett.*, **25**, 1415 (2000).
4. Bagayev S.N., Dmitriyev A.K., Chepurov S.V., Dychkov A.S., Klementyev V.M., Kolker D.B., Kuznetsov S.A., Matyugin Yu.A., Okhapkin M.V., Pivtsov V.S., Skvortsov M.N., Zakharyash V.F., Birks T.A., Wadsworth W.J., Russell P.St.J., Zheltikov A.M. *Laser Phys.*, **11** (12), 1270 (2001).
5. Kobtsev S.M., Kukarin S.V., Fateev N.V. *Kvantovaya Elektron.*, **32**, 11 (2002) [*Quantum Electron.*, **32**, 11 (2002)].
6. Dianov E.M., Kryukov P.G. *Kvantovaya Elektron.*, **31**, 877 (2001) [*Quantum Electron.*, **31**, 877 (2001)].

7. Bagayev S.N., Chepurov S.V., Klementyev V.M., Kuznetsov S.A., Pivtsov V.S., Pokasov V.V., Zakharyash V.F. *Appl. Phys. B*, **70**, 375 (2000).
8. Rytov S.M. *Vvedenie v statisticheskuyu radiofiziku* (Introduction to Statistic Radiophysics) (Moscow: Nauka, 1966).
9. Eliyahu D., Salvatore R.A., Yariv A. *J. Opt. Soc. Am. B*, **13**, 7 (1996).
10. Fuss I.G. *IEEE J. Quantum Electron.*, **30**, 2707 (1994).
11. Agrawal G.P. *Nonlinear Fiber Optics* (New York: Academic Press, 1989; Moscow: Mir, 1996).
12. Hermann J. et al. *Phys. Rev. Lett.*, **88**, 17 (2002).
13. Husakou A.V., Herrmann J. *Phys. Rev. Lett.*, **87**, 20 (2001).
14. Tzoar N., Jain M. *Phys. Rev. A*, **23**, 1266 (1981).
15. Fisher R.A., Bischel W.K. *Appl. Phys. Lett.*, **23**, 661 (1973).
16. Knox W.H. et al. *Appl. Phys. Lett.*, **46**, 1120 (1985).
17. Dianov E.M. et al. *Pis'ma Zh. Eksp. Teor. Fiz.*, **41**, 242 (1985).
18. Harbold J.M., Idlay F.O., Wise F.W., Birks T.A., Wadsworth W.J., Chen Z. *Opt. Lett.*, **27**, 1558 (2002).